

Review

## Effect of Pressure on Thermal Stability of G-Quadruplex DNA and Double-Stranded DNA Structures

Shuntaro Takahashi<sup>1</sup> and Naoki Sugimoto<sup>1,2,\*</sup>

<sup>1</sup> Frontier Institute for Biomolecular Engineering Research (FIBER), Konan University, 7-1-20 Minatojima-minamimachi, Chuo-ku, Kobe 650-0047, Japan; E-Mail: shtakaha@center.konan-u.ac.jp

<sup>2</sup> Faculty of Frontiers of Innovative Research in Science and Technology (FIRST), Konan University, 7-1-20 Minatojima-minamimachi, Chuo-ku, Kobe 650-0047, Japan

\* Author to whom correspondence should be addressed; E-Mail: sugimoto@konan-u.ac.jp; Tel.: +81-774-98-2580; Fax: +81-774-98-2585.

Received: 30 August 2013; in revised form: 5 October 2013 / Accepted: 24 October 2013 /

Published: 29 October 2013

---

**Abstract:** Pressure is a thermodynamic parameter that can induce structural changes in biomolecules due to a volumetric decrease. Although most proteins are denatured by pressure over 100 MPa because they have the large cavities inside their structures, the double-stranded structure of DNA is stabilized or destabilized only marginally depending on the sequence and salt conditions. The thermal stability of the G-quadruplex DNA structure, an important non-canonical structure that likely impacts gene expression in cells, remarkably decreases with increasing pressure. Volumetric analysis revealed that human telomeric DNA changed by more than  $50 \text{ cm}^3 \text{ mol}^{-1}$  during the transition from a random coil to a quadruplex form. This value is approximately ten times larger than that for duplex DNA under similar conditions. The volumetric analysis also suggested that the formation of G-quadruplex DNA involves significant hydration changes. The presence of a cosolute such as poly(ethylene glycol) largely repressed the pressure effect on the stability of G-quadruplex due to alteration in stabilities of the interactions with hydrating water. This review discusses the importance of local perturbations of pressure on DNA structures involved in regulation of gene expression and highlights the potential for application of high-pressure chemistry in nucleic acid-based nanotechnology.

**Keywords:** DNA; G-quadruplex; high pressure; thermodynamics; volumetric analyses; hydration; molecular crowding

---

## 1. Introduction

Biomolecules form tertiary structures through noncovalent intra- or intermolecular interactions. These noncovalent interactions are weak compared with covalent bonding and can be easily perturbed by temperature changes. Like temperature, pressure is a key factor of thermodynamics. From a physico-chemical point of view, pressure effects are mainly due to impacts on volumetric aspects of the system. According to Le Chatelier's principle, the application of pressure shifts an equilibrium toward the state that occupies a smaller volume. Therefore, the properties of biomolecules like volume, compressibility, and expansibility that depend on hydration and molecular packing determine the effect of high pressure on the equilibrium between folded and unfolded states. Pressures for the analysis of biomolecule properties generally range from 0.1 MPa (atmospheric pressure) to 1 GPa. In this range, noncovalent bonding is affected, and high pressure can perturb the tertiary structure of biomolecules and cause the changes in structure or enzymatic activity. The effect of high pressure on protein structures has been relatively well characterized [1–4]. Most proteins denature or change conformation at high pressure even at low temperature. One can explain the decrease of the partial molar volume of proteins by the penetration of water molecules bound in cavities of structured proteins [5–10].

The discovery of high-pressure-induced protein unfolding and denaturation was made in 1914 [11]. It was not until 1964 that the first report of the effect of pressure on a nucleic acid secondary structure appeared [12]. The stability of nucleic acids is determined factors such as base pairing, base stacking, electrostatic interactions, the surrounded solution condition, and so on. Hydration is one of the most important factors to consider. As mentioned above, pressure largely affects the hydration of biomolecules. Analysis under high pressure can provide structural insight into hydrating water. In G-quadruplex formation hydration is a dominant factor for determination of the type of four-stranded conformation and stability. G-quadruplexes as well as other non-canonical structures of DNA (and RNA) can regulate biological processes such as transcription and translation [13,14]. Therefore the pressure effect on these structures is of interest as transient pressure differentials inside living cells might impact the stabilities of these and other non-canonical structure of nucleic acids. Furthermore, the different sensitivity of each DNA structure to pressure is possibly useful to develop nano-materials triggered by pressure effects.

In this review, we focus our attention on the effect of hydrostatic pressure on the stability of nucleic acid structures. First, we discuss previous research into the pressure effect on double-stranded DNA by using thermodynamic, kinetic, and structural analyses. Second, we discuss what is known about the pressure effect on non-canonical structures of nucleic acids, especially the G-quadruplex, and describe how high pressure study of nucleic acids may lead to control of gene expressions of cellular functions, and permit to design novel materials of nucleic acids.

## 2. Pressure Effect on Canonical Duplex of Nucleic Acids

### 2.1. Melting Analysis under High Pressure by Temperature Change

To investigate the structural stability of nucleic acids, temperature change experiments are often used because helices of DNA and RNA can reversibly unfold upon heating and refold upon cooling. Because of hypochromism, the helix form of nucleic acids has a different ultraviolet (UV) absorption (different molar extinction coefficient) from the random coil form. Analysis of the circular dichroism (CD)

spectrum over a range of temperatures is also widely used because CD is highly sensitive to the structural transitions of nucleic acids. Thus, UV and CD melting curves can be used to study the thermal stability of nucleic acids. The temperature at the midpoint of absorbance change is called melting temperature,  $T_m$ . In physical terms,  $T_m$  corresponds to the temperature at which  $\Delta G = 0$  of the equilibrium between folded and unfolded conformations of nucleic acids. When pressure is applied, the equilibrium can shift resulting in either a  $T_m$  increase or decrease. Considering the Clapeyron equation:

$$dT_m/dP = T_m \Delta V_{tr} / \Delta H \quad (1)$$

where the volumetric parameter  $\Delta V_{tr}$  [15] for formation of the folded structure of nucleic acids can be obtained from several series of  $T_m$  measurements at different pressures. To calculate the  $\Delta V_{tr}$  value,  $\Delta H$  is required.  $\Delta H$  can be calculated from the helix-coil transitions as the van't Hoff enthalpy from the optical and spectroscopic data. The value of  $\Delta H_{cal}$  obtained from calorimetry can also be utilized. When  $\Delta T_m/\Delta P$  is positive and  $\Delta H$  is negative,  $\Delta V_{tr}$  must be negative, which means the stability of nucleic acid is promoted with increasing pressure.

In the early studies, the effects of pressure on natural DNAs were investigated. Due to availability, calf thymus DNA has been analyzed intensively to study the thermodynamic parameters with changing pressure. Weida and Gill reported  $T_m$  changes of calf thymus DNA under high pressure followed using CD technique. In the presence of 30 mM NaCl, the value of  $dT_m/dP$  was  $4.49 \times 10^{-2} \text{ K} \cdot \text{MPa}^{-1}$  [15,16]. This corresponds to a  $\Delta V_{tr}$  value of  $-4.5 \text{ cm}^3 \cdot \text{mol}^{-1}$  (Table 1). Gunter and Gunter carried out similar experiments in the presence of 140 mM KCl and obtained the values of  $2.34 \times 10^{-2} \text{ K} \cdot \text{MPa}^{-1}$  and  $-2.7 \text{ cm}^3 \cdot \text{mol}^{-1}$  for  $dT_m/dP$  and  $\Delta V_{tr}$ , respectively (Table 1) [17]. Nordmeier revealed the dependency of salt concentration on the volumetric parameters [18]. In a series of KCl concentrations, the magnitude of  $\Delta V_{tr}$  increased with increasing the salt concentration (Table 1). DNA isolated from *C. perfringens* was examined by Hawley and MacLeod, who showed that the values of  $\Delta T_m/\Delta P$  were positive and increased linearly with NaCl concentration (Table 1) [19]. Thus, the structure of natural DNA was stabilized by pressure and salt. The properties of natural DNA depended on pressure in the opposite direction; protein structure is generally unfolded by pressure. For example, the  $-\Delta V_{unfolding}$  (corresponding to  $\Delta V_{tr}$  in this review) of RNase A is  $45 \text{ cm}^3 \cdot \text{mol}^{-1}$  and that for SNase is  $80 \text{ cm}^3 \cdot \text{mol}^{-1}$  [20–22]. These results mean that under pressure the volumes of these proteins (including the volume of hydration) become much larger and that their tertiary structures tend to unfold.

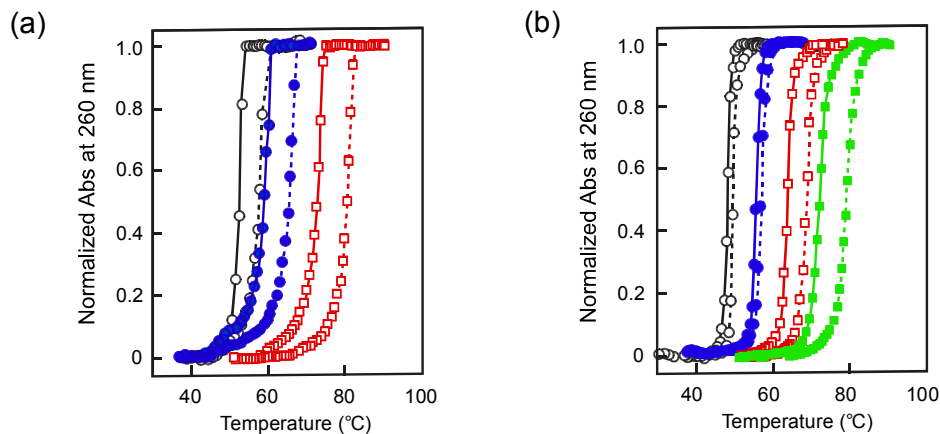
In further investigations, the effect of pressure on nucleic acids of various sequences and lengths were characterized. Macgregor *et al.* intensively investigated the effect of pressure on synthetic nucleic acids by UV melting under high pressure (Figure 1). Poly[d(A-T)] in the presence of 20 mM NaCl showed a positive value of  $\Delta T_m/\Delta P$  and a negative value of  $\Delta V_{tr}$  with a similar magnitude to that of calf thymus DNA in the presence of 5 mM KCl (Table 1) [18]. With increasing concentration of NaCl, these parameters linearly increased [23]. Salt concentration had a relatively large effect on  $\Delta T_m/\Delta P$  and  $\Delta V_{tr}$  values for poly(dA)·poly(dT) [23], suggesting that the hydration of homopolymers differed from that of natural DNA (Table 1). Although poly[d(G-C)] has a very high  $T_m$  value (over 100 °C), the use of high pressure enabled measurement of the ‘real’  $T_m$  due to the prevention of boiling. In the presence of 52 mM NaCl, the value of  $\Delta T_m/\Delta P$  was 4.8 times larger and the magnitude of  $\Delta V_{tr}$  value was 5.3 times larger than those of poly[d(A-T)] in the presence of 50 mM NaCl (Table 1) [23]. In the presence of 1 M NaCl, however, the changes in these values of poly[d(G-C)] were only 1.7 times larger than those of

poly[d(A-T)], which indicated that the salt dependence of  $\Delta V_{tr}$  for poly[d(G-C)] is smaller than that for poly[d(A-T)]. The value  $\ln K_{obs}/\ln [\text{cation}]$  is equal to the number of cations taken up during the formation of duplexes, where  $K_{obs}$  means the observed equilibrium constant for the formation of the duplex [24]. From this result, it was therefore concluded that a GC base pair binds fewer ions during folding than does an AT base pair.

**Table 1.** Pressure effect of melting temperature and volumetric parameters on natural and synthetic DNAs.

DNA	Salt Concentration	$\Delta T_m/\Delta P$ ( $10^{-2} \text{ K MPa}^{-1}$ )	$\Delta V_{tr}$ ( $\text{cm}^3 \text{ mol}^{-1}$ )	Ref.
Calf thymus	[NaCl] = 30 mM	4.49	−4.5	[16]
	[KCl] = 140 mM	2.34	−2.7	[17]
	[KCl] = 5 mM	0.46	−0.51	[18]
	[KCl] = 20 mM	1.4	−1.58	
	[KCl] = 50 mM	2.0	−2.27	
	[KCl] = 200 mM	2.9	−3.32	
	[KCl] = 500 mM	3.5	−4.02	
<i>C. perfringens</i>	[NaCl] = 10 mM	0.54		[19]
	[NaCl] = 50 mM	2.0		
	[NaCl] = 120 mM	2.6		
	[NaCl] = 360 mM	3.8		
	[NaCl] = 1.08 M	4.1		
	[NaCl] = 3.6 M	4.6		
poly[d(A-T)]	[NaCl] = 20 mM	0.36	−0.36	[23]
	[NaCl] = 50 mM	0.93	−0.90	
	[NaCl] = 200 mM	2.26	−2.14	
	[NaCl] = 1.0 M	3.86	−3.57	
poly(dA)·poly(dT)	[NaCl] = 20 mM	2.49	−2.60	[23]
	[NaCl] = 50 mM	3.15	−3.44	
	[NaCl] = 200 mM	3.86	−4.59	
poly[d(G-C)]	[NaCl] = 52 mM	4.51	−4.80	[24]
	[NaCl] = 107 mM	4.79	−5.16	
	[NaCl] = 300 mM	5.01	−5.50	
	[NaCl] = 1.0 M	6.41	−6.03	
poly(rA)·poly(rU)	[K <sup>+</sup> ] = 50 mM	−1.07	0.96	[25]
poly[d(I-C)]	[NaCl] = 75 mM	0.28	−0.26	[26]
	[NaCl] = 270 mM	1.36	−1.25	
	[NaCl] = 1.0 M	2.64	−2.39	

**Figure 1.** Normalized UV melting curves at different NaCl concentrations; solid lines are data at 0.1 MPa and dashed lines are at 200 MPa [23]. (a) Poly(dA)·poly(dT): 20 mM (○, black); 50 mM (●, blue); 200 mM (□, red). (b) Poly[d-(A-T)]: 20 mM (○, black); 50 mM (●, blue); 200 mM (□, red); 1 M (■, green).



The RNA duplex with AU base pairs is slightly destabilized upon pressuring. In the presence of 50 mM  $K^+$ , poly(rA)·poly(rU) had a  $\Delta T_m/\Delta P$  of  $-1.07 \times 10^{-2} \text{ K} \cdot \text{MPa}^{-1}$  and a  $\Delta V_{tr}$  of  $0.96 \times 10^{-2} \text{ K} \cdot \text{MPa}^{-1}$  (Table 1) [25]. Poly[d(I-C)], containing non-canonical base inosine behaves similarly to poly[d(A-T)] with a positive  $\Delta T_m/\Delta P$  and a negative  $\Delta V_{tr}$  value (Table 1) [26] although the magnitude of the values are smaller. In contrast, a methylphosphonate oligonucleotide, in which the charged oxygen of the phosphate group is replaced by uncharged methyl group, showed significant increase of  $\Delta T_m/\Delta P$  [26]. These data emphasize that hydrating water has a prominent effect on the transition volume of nucleic acid unfolding processes.  $\Delta V_{tr}$  can be described as follows:

$$\Delta V_{tr} = \Delta V_M + \Delta V_T + \Delta V_I \quad (2)$$

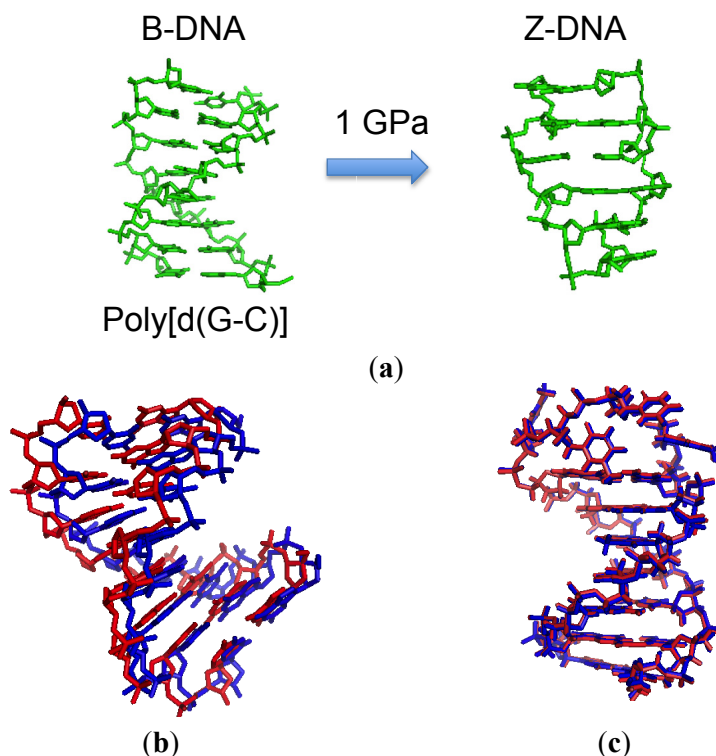
where  $\Delta V_M$  is intrinsic volume change of the DNA,  $\Delta V_T$  is thermal volume change indicating the change of the void space of the DNA,  $\Delta V_I$  is interaction volume change (*i.e.*, hydration volume change) [27].  $\Delta V_M$  and  $\Delta V_T$  basically depend on the structure of nucleic acids but  $\Delta V_I$  is very sensitive to the number and condition of hydration. RNA and modified nucleic acid can be a negative  $\Delta V_{tr}$  because of a different contribution of  $\Delta V_I$  from that of DNA.

## 2.2. Effect of High Pressure on the Conformation of a Duplex

The type of conformation adopted by double-stranded DNA depends on the solvent conditions. B-form DNA changes to A-form in low concentrations of salt or in hydrophobic conditions. The alternate repeat of purine and pyrimidine base pairs forms a left-handed helix, or Z-DNA, in the presence of high concentrations of salt. As shown above, pressure effect on thermodynamics for the nucleic acids largely depends on hydration and salt conditions. This suggests that pressure could induce conformational changes. The B-Z transition was the first of this type of change observed under high pressure (Figure 2a). Kryzysaniak *et al.* showed that poly[d(G-C)], which is B-form at atmospheric pressure, adopted the Z-form under 1 GPa [28]. They directly monitored the conformational change by using CD spectroscopy with pressuring up to 1 GPa. The conformational changes were monitored by CD spectra which showed

a negative Compton effect at 295 nm for Z-DNA. Such a high pressure induces lowering of molecular volume of water from a tetrameric to an octameric form due to shortening of the hydrogen bond (H-bond) distance [29,30]. The structure of water under high pressure resembles that in high salt concentration where Z-DNA is stabilized [31]. This suggested that water under high pressure preferred to interact with phosphate groups of DNA chains located in the groove of Z-DNA. The conformation of the methylated form of poly[d(G-C)] was also investigated under pressure. The transition was not observed under high pressure, although it does occur at atmospheric pressure due to the lower flexibility of methylated nucleotide. In the case of RNA, A-Z transitions of r(GC)<sub>6</sub> and r(AU)<sub>6</sub> are observed at 600 MPa in the presence of 5 M NaCl. The concentration of salt required to induce the A-Z transition in RNA is higher than that for poly[d(G-C)], because water binds tightly to the RNA backbone because there are the 2'-OH group [32]. Thus, high pressure can induce Z-form of nucleic acid by the perturbation of the conformation of water molecules, but the flexibility of nucleic acid backbone restricts the effect of high pressure on the structural change.

**Figure 2.** Pressure-induced structural changes to the DNA duplex. (a) B-Z transition confirmed by CD spectroscopy; (b) Structure of DNA duplex visualized by X-ray crystallography at atmospheric pressure (red) and at 1.39 GPa (blue); (c) Structure of DNA hairpin visualized by NMR at 3 MPa (red) and at 200 MPa (blue).



A few studies have reported the structure of DNA helix under high pressure determined by using X-ray crystallography or NMR. Girard *et al.* prepared crystals of d(GGTATACC), which forms a self-complementary duplex, and the high-resolution structure was analyzed under 0.55, 1.09, and 1.39 GPa of pressure (Figure 2b) [33]. The crystal structure revealed that the middle of the duplex adopted the A-form, whereas the edges of the duplex formed a disordered B conformation. The spacing

of stacked bases shortened by 0.15 Å/GPa and A-DNA hydrogen bonding also shortened by 0.04 Å/GPa. This is in contrast to effects of pressure on bonds in proteins; in proteins, salt bridges and H-bond lengths are usually shortened by  $\sim 0.1$  Å/GPa [34–36]. These differences indicated that the adaptation of DNA to high pressure could be achieved by small variations of arrangements along the backbone. As pressure increases, the first shell of hydration is gradually compressed, but the pentagonal network of water molecules found in major groove is not disrupted. Thus, all the Watson-Crick base pairs and hydrogen networks within major grooves are preserved, which enables the DNA duplex to remain structured at even very high pressure.

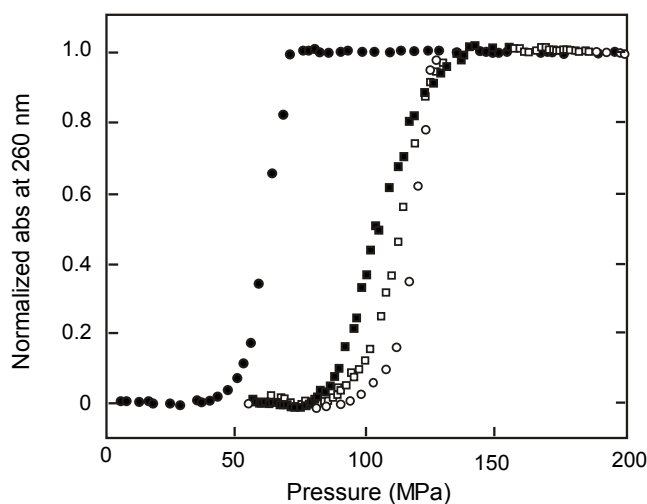
NMR analysis is a powerful technique for study of the effects of pressure on the structure of nucleic acids. NMR under high pressure [37–39] was used to investigate the structure of B-DNA (Figure 2c) [40]. The hairpin DNA d(CTAGAGGATCCTUTTGGATCCT) was used, and only the stem region was analyzed. Under 200 MPa, chemical shifts indicated a change in structure of 0.17 Å root mean square relative to the conformation at atmospheric pressure, which is at the lower end of the range of structural changes seen in proteins [37–39]. Only 0.042% reduction in volume was observed, corresponding to an intrinsic compressibility of  $0.6 \times 10^{-4}$  mL·mol<sup>-1</sup>·bar<sup>-1</sup> per nucleotide. This value is very small compared to typical adiabatic molar compressibility measured for DNA solutions ( $30\text{--}70 \times 10^{-4}$  mL·mol<sup>-1</sup>·bar<sup>-1</sup>), suggesting that the compressibility of DNA comes from not DNA molecule itself but from the hydration layer surrounding DNA [41]. The biggest change was an increase of the width in the minor groove, suggesting that the hydrating water along the minor groove adopts a different structure with lower partial volume as pressure is increased. In general, the lengths of H-bonds between Watson-Crick base pairs were also reduced. The spacing between AT pairs is 2.6 times more sensitive to the pressure than that of GC pairs. This might be derived from the different numbers of H-bonds in the pairs. The overall length of the stem was slightly increased (1.2%) at high pressure, due to a slight slide of base pairs relative to each other. A structure obtained using X-ray crystallography at high pressure showed a significant reduction in stacking distance. The conflicting results on the effect of base stacking between the crystallography and NMR awaits further investigation. FT-IR technique has also been used to investigate the structural perturbation at high pressure. The IR spectra of poly(dA)·poly(dT) was recorded at 28 °C at up to 1.2 GPa [42]. Although some shifts of prominent band were observed due to the increase of hydration and base stacking, overall the structure was B-form. Therefore, except for the specific sequence under specific conditions, the structure of B-DNA endures perturbation by high pressure. The structure is slightly but certainly affected by pressure: H-bond lengths are shortened and the distance between stacked bases are increased or decreased. The hydration layer is also compressed, and high pressure can induce structural changes to water itself, which better suits the Z-form conformation.

### 2.3. Melting of Duplex Induced by Pressure

The melting and reannealing of duplex nucleic acids is important in reactions in living cells such as replication, transcription, and translation. In nanotechnology, nucleic acid nanodevices are generally based on the control of the stability of duplexes. As shown above, in general DNA polymer duplexes have positive  $\Delta T_m/\Delta P$  and are stabilized under high pressure. If the value of  $\Delta T_m/\Delta P$  is negative, it is possible that applying pressure will induce melting of nucleic acid structure.

As shown in Table 1, the heteroduplex of poly(dA)·poly(rU), a DNA/RNA hybrid, has a negative value of  $\Delta T_m/\Delta P$  in the presence of 50 mM KCl [25]. At neutral pH and in low salt (28 mM Na<sup>+</sup>), this duplex melted sharply with a  $T_m$  of 31 °C under atmospheric pressure [43]. As pressure was increased at 25 °C, the UV absorption at 260 nm of poly(dA)·poly(rU) increased beginning at around 50 MPa (Figure 3). At 20 °C, the increase of UV absorption began at about 100 MPa. These results suggest that the profile of the UV absorbance showed a hypochromic effect with increasing pressure due to the induction of the transition of poly(dA)·poly(rU) between the duplex and the coil form. Similar results were obtained from the analysis of poly[d(A-T)] and poly[d(I-C)], which showed low  $T_m$  values of 36.0 °C and 29.0 °C at neutral pH in 5.2 mM Na<sup>+</sup> solution under atmospheric pressure, and could be melted by increasing pressure [44]. Dubins *et al.* [45] simulated the coil-to-helix transition of nucleic acids from the  $\Delta G(P, T)$  phase diagram; these calculations predicted destabilization of poly(dA)·poly(rU), poly[d(A-T)], and poly[d(I-C)] as pressure increased. The melting induced by pressure change is observed only for these specific polymers. For example, the oligonucleotides (dA)<sub>n</sub>(dT)<sub>n</sub> (where  $n = 11, 15,$  and  $19$ ), which were predicted to be sensitive to pressure melting [46], did not show transitions as pressure was increased. There have been no examples melting of DNA oligonucleotide duplexes by pressure. The existing data do suggest that pressure could affect some reactions of a genomic DNA. For example, the transcription may be started at a region along the genomic DNA partially melted by pressure. Pressure may also be useful in nanomaterials made with nucleic acids.

**Figure 3.** Pressure-induced melting of DNA duplex of poly(dA)·poly(rU) at 20 °C (○) and 25 °C (pH 6.7, 28 mM Na<sup>+</sup>) (●); poly(dAdT)·poly(dAdT) at 25 °C (pH 6.7, 5.2 mM Na<sup>+</sup>) (■); and poly(dIdC)·poly(dIdC) at 25 °C (pH 6.7, 5.2 mM Na<sup>+</sup>) (□) [43,44].



#### 2.4. Kinetic Analyses

Kinetic analyses of the coil-to-helix transitions provide informative insights into the mechanism of helix formation and melting regulated with pressure. Analysis of the hysteresis observed during UV annealing and melting processes is convenient for characterization of the kinetic properties of duplex formation (Figure 4a). The forward rate constant  $k_1$  (for the formation reaction) and the reverse rate



constant  $k_{-1}$  (for the melting reaction) can be calculated from the absorbance and temperature changes with time [47]. The rate can be described as:

$$k = \exp\{(-\Delta V^\ddagger/RT)P\} \quad (3)$$

where  $R$  is gas constant [46]. By substituting  $k_1$  or  $k_{-1}$  into Equation (2), the activation volume  $\Delta V^\ddagger_1$  for the forward step or  $\Delta V^\ddagger_{-1}$  for the reverse step can be obtained, respectively. Upon application of pressure,  $k_1$  becomes larger and  $k_{-1}$  smaller, resulting in the negative value of  $\Delta V^\ddagger_1$  and positive value of  $\Delta V^\ddagger_{-1}$ , respectively [48–51]. These results suggested that an increase in base stacking induced by higher pressure accelerated the helix formation. The activation volumes also showed dependency on GC content of the strands. For 22-mer homopurine-homopyrimidine oligonucleotides [48], increasing the fraction of GC base pairs from 0.14 to 0.5 causes  $\Delta V^\ddagger_1$  to increase by a factor of three, whereas the value of  $\Delta V^\ddagger_{-1}$  became 10 times smaller (Table 2). Furthermore, the subtraction of  $\Delta V^\ddagger_{-1}$  from  $\Delta V^\ddagger_1$  gives the transition volume  $\Delta V_{tr \text{ kinetic}}$ , which is equivalent to  $\Delta V_{tr}$  obtained from the Clapeyron equation [Equation (1)]. Indeed, volumetric parameters obtained by the two methods are in agreement.

**Figure 4.** (a) UV melting curves of 22-mer DNA used in [43]. The blue triangle and red closed circle represent annealing and melting process, respectively; (b) Transition volumes for each of six independent dinucleotide steps plotted as a function of the change in their solvent accessible surface area,  $\Delta S_A$  [46].

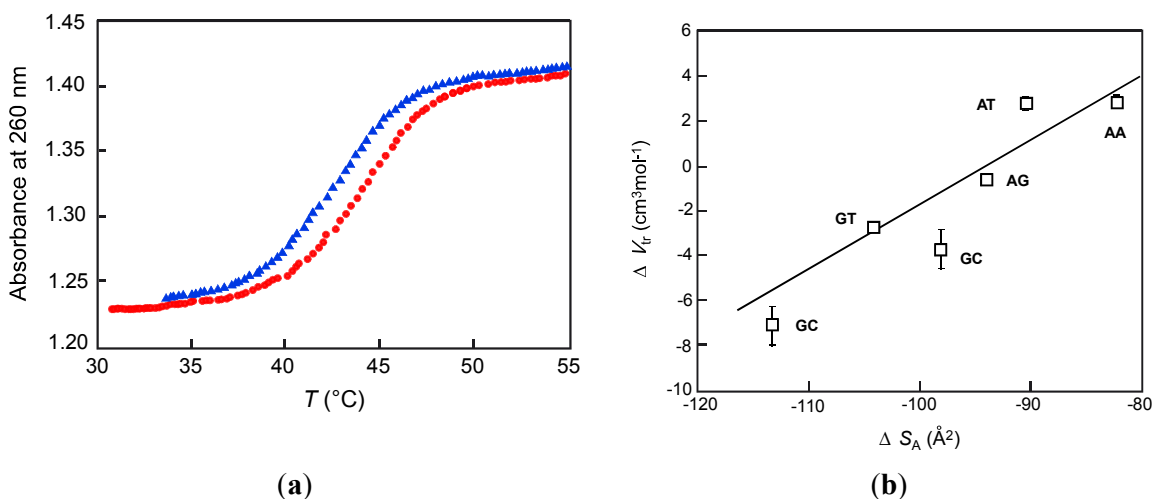


**Table 2.** Activation volume of 22-base duplexes in the presence of 20 mM NaCl [43].

Fraction of GC	$\Delta V^\ddagger_1$ ( $\text{cm}^3 \text{mol}^{-1}$ )	$\Delta V^\ddagger_{-1}$ ( $\text{cm}^3 \cdot \text{mol}^{-1}$ )	$\Delta V_{tr \text{ kinetic}}$ ( $\text{cm}^3 \text{mol}^{-1}$ ) <sup>a</sup>	$\Delta V_{tr}$ ( $\text{cm}^3 \text{mol}^{-1}$ ) <sup>b</sup>
0.5	-6.7	1.6	-8.3	-5.8
0.32	-8.0	0.40	-8.4	-8.0
0.23	-13	15	-28	-13
0.14	-20	17	-37	-20

<sup>a</sup>  $\Delta V_{tr \text{ kinetic}}$  calculated using the activation volumes; <sup>b</sup>  $\Delta V_{tr}$  calculated using the Clapeyron equation (Equation (1)). The values given here are estimated to have the errors within  $\pm 15\%$ .

Dubins and Macgregor examined the nearest-neighbor effect on the kinetics of the duplex formation under high pressure [51]. The nearest-neighbor model is based on the assumption that the stability of a nucleic acid duplex is determined by type of base pair and the adjacent base pairs, enabling prediction of the thermal stability of a duplex from sequence [52–54]. The activation volume ( $\Delta V_{\ddagger_1}$  and  $\Delta V_{\ddagger_{-1}}$ ), the estimated transition volume  $\Delta V_{\text{tr kinetic}} (= \Delta V_{\ddagger_1} - \Delta V_{\ddagger_{-1}})$ , and the transition volume calculated by Clapeyron equation (Equation (1))  $\Delta V_{\text{tr}}$  were determined for a 22-mer DNA duplex. For volumetric properties, the model that emphasizes the nature of the two bases in each dinucleotide step but does not distinguish the order (*i.e.*, 5'-AC-3' and 5'-CA-3' are equivalent) was most appropriate. This trend can be explained if this property is dominated by the contribution of size of the dinucleotide step. Solvent accessible surface area,  $\Delta S_A$ , is widely used to characterize the surface size of a molecule accessible by solvent molecules [55–58]. Indeed, the  $\Delta S_A$  values of each base pair revealed a good correlation with of  $\Delta V_{\text{tr}}$  values of the duplex (Figure 4b). Thus, kinetic analyses provide the activation volumes of the formation and melting of coil-to-helix transition of nucleic acids. By analysis of these parameters, it was concluded that hydrating water and interactions between nucleotide bases and sizes of bases contribute to annealing and melting reactions of nucleic acids.

### 2.5. Effect of Pressure on the Interactions between DNA and Protein

Reactions that occur along DNA (or RNA) such as replication, transcription, and recombination are carried out by numerous proteins and enzymes. During the recognition process between nucleic acid and protein electrostatic interactions, conformational changes, and hydration changes may occur. Therefore, it was hypothesized that pressure can regulate the interaction between protein and DNA, and that study of the effects of pressure will provide thermodynamic information on the reaction. Restriction endonucleases, which are an excellent model of DNA interacting proteins, have reduced ability to bind and hydrolyze DNA under high pressure, but the specificity of the reaction is enhanced [59,60]. High pressure may promote hydration of the enzyme and the enzyme-DNA interface [61], weakening non-specific interactions more than specific ones. LacI repressor protein adopts a tetrameric conformation that is destabilized in the presence of DNA at high pressure [62]; in contrast, dimerization of LexA repressor is stabilized upon DNA binding at high pressure due to effects of the condensation of each monomer on DNA [63]. Recently, the effects of pressure and temperature on the binding of RecA to a single-stranded DNA were investigated [64]. A phase diagram of  $\Delta G(P, T)$  of formation of a RecA-DNA complex was obtained that indicated that the dissociation of the complex depended on the stability of RecA protein rather than DNA. This result agreed well with the structural analysis of DNA under high pressure described above [33,40]. Pressure can perturb the interaction between DNA and its cognate protein by changing the hydration in the protein, but there are no reports about the pressure perturbation to DNA-protein interaction due to the physical alterations of nucleic acid properties by pressure.

## 3. Non-Canonical Structures of Nucleic Acids under High Pressure

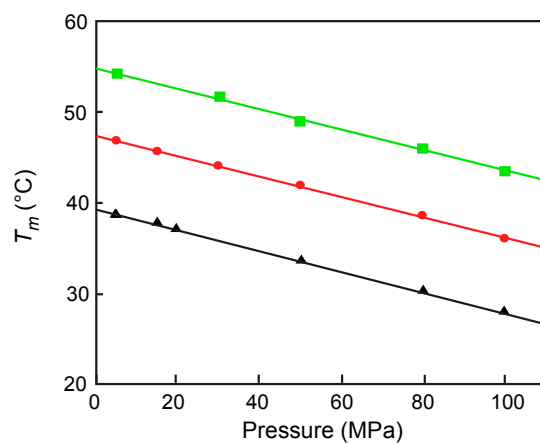
### 3.1. G-Quadruplex

The canonical structure of nucleic acids is a duplex stabilized by Watson-Crick base pairing. Various non-canonical structures of nucleic acids have been identified and there is a growing body of evidence

that these structures are adopted under certain conditions by genomic DNAs and transcribed RNAs in living cells. The G-quadruplex has received significant attention [65]; it is formed by stacking of guanine quartets (G-quartets), four guanine bases in a coplanar arrangement stabilized by Hoogsteen base pairing [66–68]. Although G-quadruplex structures are polymorphic depending on the sequence, metal ions, and the cosolute [69–72], all G-quadruplex structures have stacks of G-quartets and a central cavity that binds a monovalent cation, such as  $K^+$  or  $Na^+$ , through interactions with the O6 carbonyls of the guanines [73]. The G-quadruplex can be intra- or intermolecularly, and exhibits a much more compact conformation than single-stranded nucleic acids [74]. Sequences with the potential to form G-quadruplex structures are located throughout the genome [75,76], and G-quadruplex structures appear to be involved in the regulation of gene expression, which includes not only telomere maintenance but also regulation of transcription, recombination, replication, and translation [14,77–85]. Key factors for the stabilization of G-quadruplexes are the incorporation of a monovalent cation, the number of G-quartets, and the lengths of loops [86,87], but the major force determining the stability of a G-quadruplex is hydration [88–91]. Unlike folding of a nucleic acid duplex, water molecules are released during the folding of G-quadruplex [90,91]. Therefore, volumetric analysis using high pressure has proven very useful for analysis of the mechanism of folding and unfolding of G-quadruplexes.

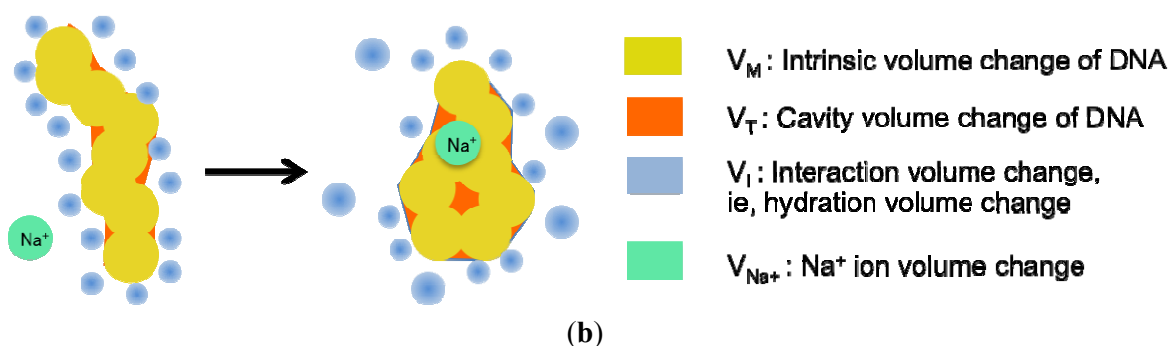
There are two excellent reports of the study of G-quadruplex structures under high pressure. The first was reported by Chalikian's group [92]. This group studied the human telomeric (H-telo) oligonucleotide, d[A(GGGTTA)<sub>3</sub>GGG]. H-telo DNA forms a basket type G-quadruplex characterized by an antiparallel structure with one diagonal and two lateral loops [93]. The authors conducted UV melting under high pressure to monitor the unfolding process of H-telo oligonucleotide in the presence of  $Na^+$  ions. With increasing pressure, the melting temperature was remarkably decreased, indicating that  $\Delta T_m/\Delta P$  was less than  $-10 \times 10^{-2} \text{ K}\cdot\text{MPa}^{-1}$  (Figure 5a).

**Figure 5.** (a) Dependencies of the  $T_m$  for G-quadruplex DNA on pressure in the presence of 20 mM ( $\blacktriangle$ ), 50 mM ( $\bullet$ ), and 100 mM ( $\blacksquare$ ) NaCl [92]; (b) Graphical image of volumetric change of G-quadruplex based on Equation (4).



(a)

Figure 5. Cont.



Using the Clapeyron equation the transition volume,  $\Delta V_{tr}$ , was determined to be  $68 \text{ cm}^3 \cdot \text{mol}^{-1}$  in the presence of 20 mM  $\text{Na}^+$  ion. An increase in the concentration of NaCl to 100 mM was accompanied by a decrease of  $\Delta V_{tr}$  from 68 to  $56 \text{ cm}^3 \cdot \text{mol}^{-1}$  (Table 3). These values indicate that the structure of the H-telo oligonucleotide is destabilized under high pressure, opposite of the thermostability of canonical duplexes, and that the change in volume is much larger than that of any other oligonucleotide structure characterized.

In order to estimate the contribution of the hydrating water in the transition of H-telo G-quadruplex, an approximate algorithm was presented. The change in volume associated with G-quadruplex formation  $\Delta c_{tr}$  determined experimentally can be summarized derived from Equation (2) as follows:

$$\Delta V_{tr} = \Delta V_M + \Delta V_T + \Delta V_I + \Delta V_{\text{Na}^+} \quad (4)$$

where  $\Delta V_M$  is intrinsic volume change of the DNA,  $\Delta V_T$  is thermal volume change indicating the change of the void space of the DNA,  $\Delta V_I$  is interaction volume change (*i.e.*, hydration volume change), and  $\Delta V_{\text{Na}^+}$  is the volume change of incorporated sodium ion. By using molecular dynamics simulations of NMR structure of H-telo DNA (Figure 5b) [93], solvent-accessible surface area was estimated [56–59]. By using the empirical estimation of the thickness of the thermal volume and the known parameter of partial molar volume contribution of sodium ion [94–97],  $\Delta V_M$ ,  $\Delta V_T$ , and  $\Delta V_{\text{Na}^+}$  were estimated to be  $233 \text{ cm}^3 \text{ mol}^{-1}$ ,  $-370 \text{ cm}^3 \text{ mol}^{-1}$ , and  $-17.7 \text{ cm}^3 \text{ mol}^{-1}$  (three  $\text{Na}^+$  ions), respectively. A  $\Delta V_{tr}$  value of  $67 \text{ cm}^3 \text{ mol}^{-1}$  was obtained from vibration tube densitometry. Therefore,  $\Delta V_I$  was estimated from Equation (3) as  $186 \text{ cm}^3 \text{ mol}^{-1}$  at 25 °C.  $\Delta V_I$  reflects water expansion around polar and charged groups of DNA during transition and is presented as:

$$\Delta V_I = n_h (V_h - V_0) \quad (5)$$

where  $n_h$  is the number of waters of hydration,  $V_h$  is the change in partial molar volume of water of hydration, and  $V_0$  is the change in bulk water. By using  $-1.8 \text{ cm}^3 \text{ mol}^{-1}$  as the value of  $(V_h - V_0)$  [98], a release of 103 water molecules occurs during the folding of H-telo DNA, which corresponds to about 18% of the net hydration of the coil formation.

Another study from our group focused on the effect of molecular crowding conditions on G-quadruplex stability under high pressure [99]. Molecular crowding occurs in the presence of cosolute such as poly(ethylene glycol) (PEG) and mimics the conditions inside cells [100–102]. We have reported that crowding reagents like PEG stabilize G-quadruplexes due to changes in water activity and DNA hydration [90,103,104]. Chalikian's group found that changes in hydration accompany the transition

from coil to quadruplex [92]. It is possible that the volumetric characteristics of G-quadruplex DNA are also affected by molecular crowding agents.

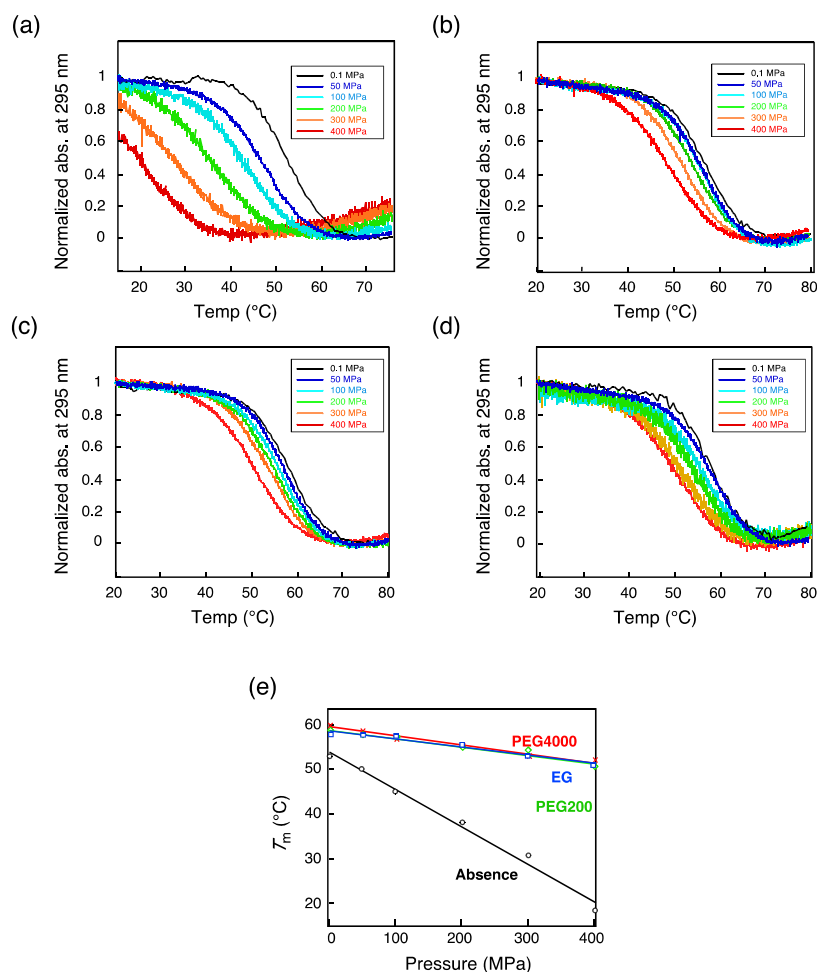
**Table 3.** The value of the molar volume change  $\Delta V_{tr}$  of the transition for G-quadruplex DNA.

DNA	Salt or Cosolute	$\Delta V_{tr}$ ( $\text{cm}^3 \text{mol}^{-1}$ )
H-telo <sup>a</sup>	[NaCl] = 20 mM	68 ± 2
	[NaCl] = 50 mM	60 ± 2
	[NaCl] = 100 mM	56 ± 2
TBA <sup>b</sup>	(Absence)	54.6 ± 4.2
	40 wt% Ethylene glycol	12.5 ± 0.8
	40 wt% PEG 200	12.9 ± 0.9
	40 wt% PEG 4000	13.1 ± 1.0

<sup>a</sup> Each solution was buffered with 10 mM sodium phosphate (pH 7.0), 0.1 mM EDTA, 0.1 mM  $\text{NaN}_3$ , and each NaCl concentration [92]; <sup>b</sup> Each solution was buffered with 30 mM Tris-HCl (pH 7.0) and 100 mM KCl [100].

In our study, we used the thrombin binding aptamer (TBA; 5'-GGTTGGTGTGGTTGG-3') [105], which folds into an intramolecular, antiparallel G-quadruplex structure in the presence of various monovalent and divalent cations and cosolutes [88,90]. Temperature-dependent UV melting under high pressure was analyzed first in the presence of 100 mM KCl. In the absence of cosolute (PEG), the thermal stability was decreased with increasing pressure up to 400 MPa (Figure 6a) as observed for the H-telo DNA [92]. In contrast, in the presence of 40 wt% PEG, little unfolding of the TBA DNA was observed even under high pressure (Figure 6b–d). Our thermodynamic analysis indicated that crowding conditions repress the pressure effect due to enthalpic contributions. A volumetric analysis using the Clapeyron equation revealed that, in the absence of cosolute,  $\Delta T_m/\Delta P$  was  $-8.4 \times 10^{-2} \text{ K MPa}^{-1}$  and  $\Delta V_{tr}$  was  $54.6 \text{ cm}^3 \text{ mol}^{-1}$ , whereas in the presence of ethylene glycol, another crowding agent,  $\Delta T_m/\Delta P$  was  $-1.9 \times 10^{-2} \text{ K MPa}^{-1}$  and  $\Delta V_{tr}$  was  $12.5 \text{ cm}^3 \text{ mol}^{-1}$  (Figure 6e, Table 3). PEG200 and PEG4000 (PEGs with average molecular weights of 200 and 4,000, respectively) caused effects similar to that of ethylene glycol (Table 3). We hypothesize that the crowding reagents did not affect the structure-dependent volume of TBA DNA and that  $\Delta V_M$ ,  $\Delta V_T$  and  $\Delta V_{K^+}$  are the same in the absence or presence of crowding reagents. Thus,  $\Delta V_I$  reflects the effect of high pressure in the presence of cosolute. Considering the tiny decrease of bulk water volume  $V_0$  in the presence of ethylene glycol or PEG [106,107], the Equation (5) indicates that the cosolute may decrease the number of hydration water ( $n_h$ ) and/or increase radii of hydrating waters to expand its volume ( $V_h$ ). Ethylene glycol or poly(ethylene glycols) decreases the volume change of the transition by one fourth due to the alteration of the number and/or radii of hydrating waters. The observed structural switching of DNA induced by pressure and cosolutes suggests that some gene expression may be regulated quadruplex by pressure changes in living cells.

**Figure 6.** Effect of cosolute on the transition of 40  $\mu\text{M}$  TBA from a quadruplex to a coil under various pressures [99]. UV melting curves were obtained (a) in the absence of cosolute or in the presence of (b) 40 wt% ethylene glycol, (c) 40 wt% PEG200, and (d) 40 wt% PEG4000. The changes of absorbance at 295 nm were analyzed under atmospheric pressure (0.1 MPa, black), 50 MPa (blue), 100 MPa (light blue), 200 MPa (green), 300 MPa (orange), and 400 MPa (red). Each solution was buffered with 30 mM Tris-HCl (pH 7.0) and contained 100 mM KCl. (e) Dependencies of the  $T_m$  for G-quadruplex DNA on pressure in the presence of ethylene glycol (blue), PEG200 (green), PEG4000 (red), and in the absence of cosolute (black).



### 3.2. Triple Helix

An oligonucleotide duplex can incorporate another strand via Hoogsteen base pairing to form a triple helix, also called a triplex. Wu and Macgregor examined the thermal stability of poly(dA)·poly(dT)<sub>2</sub> under high pressure [23]. In the presence of 2 M NaCl, the triplex had a  $\Delta T_m/\Delta P$  value of  $4.50 \times 10^{-2} \text{ K MPa}^{-1}$  and relatively large magnitude  $\Delta V_{tr}$  ( $-7.81 \text{ cm}^3 \text{ mol}^{-1}$ ). These parameters are obviously higher than those of poly(dA)·poly(dT) duplex. Thus, this result indicated that high pressure effectively stabilizes the triplex more than the duplex. An increase in the concentration of NaCl up to 3 M increased these parameters:  $\Delta T_m/\Delta P$  was  $5.80 \times 10^{-2} \text{ K MPa}^{-1}$  and  $\Delta V_{tr}$  was  $-10.4 \text{ cm}^3 \text{ mol}^{-1}$ . A kinetic analysis of the

triplex formation was also reported [49]. The rate of  $k_{-1}$  for the unfolding process for the DNA triplex was affected by pressure more than was the rate of DNA duplex dissociation [48]. The activation volume for the triplex dissociation  $\Delta V_{-1}^{\ddagger}$  was remarkably large at  $+39.9 \text{ cm}^3 \text{ mol}^{-1}$  [48]. These values were determined in a different buffer than used for analysis of the duplex and so cannot be directly compared.

### 3.3. Hairpin DNA

Hairpin DNAs or RNAs form intramolecularly and consist of a stem of Watson-Crick base pairs and a loop. The stability of a hairpin is determined by mainly by the sequence and number of base pairs within the stem region, but is affected by the loop sequence and by whether metal ions are bound [108–111]. Amiri and Macgregor investigated the stability of DNA hairpins under high pressure and determined volumetric parameters of hairpin DNAs containing different nucleation stacks and loop sequences. The systematic analysis revealed that the  $\Delta V_{\text{tr}}$  values of transition of coil-to-helix were as small as those of duplex but some  $\Delta V_{\text{tr}}$  values became positive at low sodium ion concentrations (Table 4).

**Table 4.** Transition temperatures ( $T_m$ ) at atmospheric pressure and the molar volume change of the transition for the hairpin DNA with each loop sequence.

Nucleation stack	Loop sequence						
	Na <sup>+</sup> (mM)	TA <sub>2</sub> T		TG <sub>2</sub> T		TC <sub>2</sub> T	
		$T_m$ (°C)	$\Delta V_{\text{tr}}$ (cm <sup>3</sup> mol <sup>-1</sup> ) <sup>a</sup>	$T_m$ (°C)	$\Delta V_{\text{tr}}$ (cm <sup>3</sup> mol <sup>-1</sup> ) <sup>a</sup>	$T_m$ (°C)	$\Delta V_{\text{tr}}$ (cm <sup>3</sup> mol <sup>-1</sup> ) <sup>a</sup>
AT/AT	10	42.1	0.44	42.8	1.41	44.9	-1.81
	20	43.2	-0.18	44.0	0.25	46.1	-2.27
	50	44.6	-0.83	45.5	1.55	48.7	-3.05
	100	46.1	-1.46	46.8	-2.89	51.3	-3.76
AA/TT	10	40.2	1.96	37.9	2.35	44.0	-0.78
	20	41.5	1.15	41.1	0.86	45.4	-1.18
	50	43.3	0.19	43.5	-0.85	47.9	-1.75
	100	44.7	-0.74	45.1	-2.14	49.9	-2.35

<sup>a</sup> The error was less than  $\pm 0.32 \text{ cm}^3 \text{ mol}^{-1}$ .

For example, the DNA having TC<sub>2</sub>T loop with AA/TT nucleation stack (5'-GGATAATCCTTTAT CC-3') had a negative  $\Delta e_{\text{tr}}$  value of  $-0.78 \text{ cm}^3 \text{ mol}^{-1}$  in the each concentration of Na<sup>+</sup> ion, whereas that with the TG<sub>2</sub>T loop with the same nucleation stack had a positive  $\Delta V_{\text{tr}}$  of  $2.35 \text{ cm}^3 \text{ mol}^{-1}$  in the presence of 10 mM Na<sup>+</sup> ion. Considering that  $\Delta V_M$  in the equation (2) was negligible for DNA duplex [112,113],  $\Delta V_T$  and  $\Delta V_I$  are responsible for the contribution of each factor to  $\Delta V_{\text{tr}}$ . Furthermore,  $\Delta V_T$ , corresponding to the solvent accessible surface area  $S_A$  should be always negative because the coil form has a larger  $S_A$  than the helix. Therefore,  $\Delta V_I$  (hydration volume change) determines the magnitude of  $\Delta V_{\text{tr}}$ , which in turn depends on the loop sequence and nucleation bases. For example, a loop consisting of purine bases had a positive volume change at low salt. These results imply that there are some specific interactions between the loop and cations. The importance of hydration within a loop region was also demonstrated by osmotic pressure analysis, which revealed that the loop region within a G-quadruplex determines the thermodynamic stability and hydration of the structure [114].

A simulation technique was also utilized to investigate the pressure effect on the folding/unfolding of the hairpin structure. Garcia and Paschek used replica exchange molecular dynamics (REMD) simulations

to predict a pressure-temperature ( $P$ - $T$ ) free energy diagram for the RNA hairpin r(GCUUCGGC) and found that the RNA hairpin was destabilized by increases of pressure [115]. The change in volume was  $4.1 \text{ cm}^3 \text{ mol}^{-1}$ , which was a relatively small change compared with that of the G-quadruplex. No other sequences of RNA or DNA have been studied by simulation techniques.

#### 4. Summary and Perspectives

In summary, we have reviewed papers related to the effect of pressure on nucleic acid structural conformations and stability. Pressure acts to compress the biomolecules. Molecular volume, compressibility, and expansibility depend on hydration and molecular packing, and the partial molar volume of a biomolecule can decrease or increase upon folding. The canonical DNA duplex formed with Watson-Crick base pairs generally has a negative partial molar volume of the melting transition ( $\Delta V_{tr}$ ), which indicates that applying pressure causes the duplex to be more stable. The typical magnitude of  $\Delta V_{tr}$  for DNA duplexes is small compared with that of proteins. Only in specific cases such as poly[d(A-T)] do nucleic acid structures have a positive value of  $\Delta V_{tr}$  and can melting induced by pressure change be observed. Structural analyses revealed that the conformation and configuration of DNA duplex are not significantly perturbed under high pressure. These results agree with studies of the interactions between proteins and DNA under high pressure in which it was observed that the conformation of the protein is only affected by pressure.

In contrast to the stabilities of duplexes, which are relatively unaffected by pressure, non-canonical DNA (and RNA) structures are more sensitive to the pressure effect. G-quadruplex DNA structures are characterized by a positive and large  $\Delta V_{tr}$  value, indicating that the G-quadruplex tends to unfold with increasing pressure and is much sensitive to pressure than the duplex form of DNA. The magnitude of the  $\Delta V_{tr}$  value is generally 10 times greater than that of a duplex and more similar to magnitudes of  $\Delta V_{tr}$  measured for proteins. Other DNA structures such as a triplex and a hairpin DNA have smaller changes in volume than do the G-quadruplexes but are more sensitive to pressure than a duplex.

Osmotic pressure analysis show that DNA duplexes take up water molecules during the folding process [103,105], whereas G-quadruplexes and other non-canonical structures release water molecules [90,116,117]. The origin of different  $\Delta V_{tr}$  between DNA duplex and these structures comes from the hydration. Interestingly, the number of water molecules taken up or released does not correspond to the difference of magnitude in change of  $\Delta V_{tr}$  value. These results suggest that the physical properties of hydrating water around G-quadruplex are quite different from those of duplex. Further analysis for the hydration on non-canonical nucleic acids is needed.

Considering that G-quadruplexes and other non-canonical structures are sensitive to pressure changes, structural transitions induced by pressure may alter regulation of gene expression in cells. If local perturbations in pressure occur in cells, these changes may alter stabilities of duplex relative to non-canonical structures initiating or inhibiting cellular processes. As crowding conditions vary during the cell cycle [100], the stabilization of G-quadruplexes may depend on both cellular conditions and pressure. Recent study suggested that stress sensor protein Ras in human, which lives at atmospheric pressure, showed a relative small magnitude of transition volume of its reaction for the stress-signaling compared with those observed in G-quadruplexes [118]. And enzyme reaction such as replication and transcription may overcome the highly structured region of G-rich sequence with a help of relative low



pressure, because some enzymes translocate along DNA with disrupting the proteins bound on DNA [119]. Therefore, the effect of pressure on quadruplex DNA in living cell may happen even at relative low pressure stress, at most 100 MPa, which is an acceptable pressure for living cells on earth. To discover genetic expression systems triggered by pressure is highly interesting and desired.

Moreover, from the viewpoint of nanotechnology, DNA is a promising material for construction of sensors and nanostructures. In our previous paper [99], we utilized the property of quadruplex and duplex DNA to make switching DNA materials by pressure changes. It may be more and more possible to use pressure as a trigger to induce signals through structural changes in G-quadruplexes.

### Acknowledgments

This work was supported in part by Grants-in-Aid for Scientific Research and the MEXT-Supported Program for the Strategic Research Foundation at Private Universities (2009–2014), Japan, and the Hiraio Taro Foundation of the Konan University Association for Academic Research.

### Conflicts of Interest

The authors declare no conflict of interest.

### References and Notes

1. Meersman, F.; Dobson, C.M.; Heremans, K. Protein unfolding, amyloid fibril formation and configurational energy landscapes under high pressure conditions. *Chem. Soc. Rev.* **2006**, *35*, 908–917.
2. Silva, J.L.; Foguel, D.; Royer, C.A. Pressure provides new insights into protein folding, dynamics and structure. *Trends Biochem. Sci.* **2001**, *26*, 612–618.
3. Heremans, K.; Smeller, L. Protein structure and dynamics at high pressure. *Biochim. Biophys. Acta* **1998**, *1386*, 353–370.
4. Akasaka, K. Probing conformational fluctuation of proteins by pressure perturbation. *Chem. Rev.* **2006**, *106*, 1814–1835.
5. Hawley, S. Reversible pressure-temperature denaturation of chymotrypsinogen. *Biochemistry* **1971**, *10*, 2436–2442.
6. Frye, K.J.; Royer, C.A. Probing the contribution of internal cavities to the volume change of protein unfolding under pressure. *Protein Sci.* **1998**, *7*, 2217–2222.
7. Paliwal, A.; Asthagiri, D.; Bossev, D.P.; Paulaitis, M.E. Pressure denaturation of staphylococcal nuclease studied by neutron small-angle scattering and molecular simulation. *Biophys. J.* **2004**, *87*, 3479–3492.
8. Day, R.; García, A.E. Water penetration in the low and high pressure native states of ubiquitin. *Proteins Struct. Funct. Bioinform.* **2008**, *70*, 1175–1184.
9. Imai, T.; Sugita, Y. Dynamic correlation between pressure-induced protein structural transition and water penetration. *J. Phys. Chem. B* **2010**, *114*, 2281–2286.
10. Fabian, H.; Naumann, D. *Protein Folding and Misfolding: Shining Light by Infrared Spectroscopy*; Springer: Heidelberg, Germany, 2012.

11. Bridgman, P.W. The coagulation of albumin by pressure. *J. Biol. Chem.* **1914**, *19*, 511–512.
12. Heden, C.; Lindahl, T.; Toplin, I. The stability of deoxyribonucleic acid solutions under high pressure. *Acta Chem. Scand.* **1964**, *18*, 1150–1158.
13. Palumbo, S.L.; Ebbinghaus, S.W.; Hurley, L.H. Formation of a unique end-to-end stacked pair of G-quadruplexes in the hTERT core promoter with implications for inhibition of telomerase by G-quadruplex-interactive ligands. *J. Am. Chem. Soc.* **2009**, *131*, 10878–10891.
14. Endoh, T.; Kawasaki, Y.; Sugimoto, N. Suppression of gene expression by G-quadruplexes in open reading frames depends on G-quadruplex stability. *Angew. Chem. Int. Ed.* **2013**, *125*, 5632–5636.
15. Throughout this review, the volumetric change  $\Delta V$  ( $= \Delta V_{tr}$ ) means the value for formation of the folded conformation and the unit of pressure is MPa. Some of these values in this review were recalculated from the original values in the references.
16. Weida, B.; Gill, S. Pressure effect on deoxyribonucleic acid transition. *Biochim. Biophys. Acta* **1966**, *112*, 179–181.
17. Gunter, T.; Gunter, K. Pressure dependence of the helix-coil transition temperature for polynucleic acid helices. *Biopolymers* **1972**, *11*, 667–678.
18. Nordmeier, E. Effects of pressure on the helix-coil transition of calf thymus DNA. *J. Phys. Chem.* **1992**, *96*, 1494–1501.
19. Hawley, S.; Macleod, R. Pressure-Temperature stability of DNA in neutral salt solutions. *Biopolymers* **1974**, *13*, 1417–1426.
20. Panick, G.; Vidugiris, G.J.; Malessa, R.; Rapp, G.; Winter, R.; Royer, C.A. Exploring the temperature-pressure phase diagram of staphylococcal nuclease. *Biochemistry* **1999**, *38*, 4157–4164.
21. Panick, G.; Malessa, R.; Winter, R.; Rapp, G.; Frye, K.J.; Royer, C.A. Structural characterization of the pressure-denatured state and unfolding/refolding kinetics of staphylococcal nuclease by synchrotron small-angle X-ray scattering and Fourier-transform infrared spectroscopy. *J. Mol. Biol.* **1998**, *275*, 389–402.
22. Panick, G.; Winter, R. Pressure-Induced unfolding/refolding of ribonuclease A: Static and kinetic Fourier transform infrared spectroscopy study. *Biochemistry* **2000**, *39*, 1862–1869.
23. Wu, J.Q.; Macgregor, R.B., Jr. Pressure dependence of the melting temperature of dA-dT polymers. *Biochemistry* **1993**, *32*, 12531–12537.
24. Wu, J.Q.; Macgregor, R.B. Pressure dependence of the helix-coil transition temperature of poly [d (G-C)]. *Biopolymers* **1995**, *35*, 369–376.
25. Hughes, F.; Steiner, R. Effects of pressure on the helix-coil transitions of the poly A-poly U system. *Biopolymers* **1966**, *4*, 1081–1090.
26. Markley, J.L.; Northrop, D.B. *High Pressure Effects in Biophysics and Enzymology*; Oxford University Press: New York, USA, 1996; pp. 274–207.
27. Chalikian, T.V.; Völker, J.; Srinivasan, A.R.; Olson, W.K.; Breslauer, K.J. The hydration of nucleic acid duplexes as assessed by a combination of volumetric and structural techniques. *Biopolymers* **1999**, *50*, 459–471.
28. Krzyżaniak, A.; Salański, P.; Jurczak, J.; Barciszewski, J. B-Z DNA reversible conformation changes effected by high pressure. *FEBS Lett.* **1991**, *279*, 1–4.
29. Benson, S.W.; Siebert, E.D. A simple two-structure model for liquid water. *J. Am. Chem. Soc.* **1992**, *114*, 4269–4276.

30. Kitchen, D.B.; Reed, L.H.; Levy, R.M. Molecular dynamics simulation of solvated protein at high pressure. *Biochemistry* **1992**, *31*, 10083–10093.
31. Leberman, R.; Soper, A. Effect of high salt concentrations on water structure. *Nature* **1995**, *378*, 364–366.
32. Krzyżaniak, A.; Barciszewski, J.; Fürste, J.P.; Bald, R.; Erdmann, V.A.; Salański, P.; Jurczak, J. AZ-RNA conformational changes effected by high pressure. *Int. J. Biol. Macromol.* **1994**, *16*, 159–162.
33. Girard, E.; Prange, T.; Dhaussy, A.-C.; Migianu-Griffoni, E.; Lecouvey, M.; Chervin, J.-C.; Mezouar, M.; Kahn, R.; Fourme, R. Adaptation of the base-paired double-helix molecular architecture to extreme pressure. *Nucleic Acids Res.* **2007**, *35*, 4800–4808.
34. Fourme, R.; Ascone, I.; Kahn, R.; Girard, E.; Mezouar, M.; Lin, T.; Johnson, J.; Winter, R. New trends in macromolecular crystallography at high hydrostatic pressure. *Adv. High Press. Sci. Technol. II*; Springer : Heidelberg, Germany, 2003; pp. 161–170.
35. Girard, E.; Kahn, R.; Mezouar, M.; Dhaussy, A.-C.; Lin, T.; Johnson, J.E.; Fourme, R. The first crystal structure of a macromolecular assembly under high pressure: CpMV at 330 MPa. *Biophys. J.* **2005**, *88*, 3562–3571.
36. Li, H.; Yamada, H.; Akasaka, K. Effect of pressure on individual hydrogen bonds in proteins. Basic pancreatic trypsin inhibitor. *Biochemistry* **1998**, *37*, 1167–1173.
37. Williamson, M.P.; Akasaka, K.; Refaee, M. The solution structure of bovine pancreatic trypsin inhibitor at high pressure. *Protein Sci.* **2003**, *12*, 1971–1979.
38. Refaee, M.; Tezuka, T.; Akasaka, K.; Williamson, M.P. Pressure-Dependent changes in the solution structure of hen egg-white lysozyme. *J. Mol. Biol.* **2003**, *327*, 857–865.
39. Wilton, D.J.; Tunnicliffe, R.B.; Kamatari, Y.O.; Akasaka, K.; Williamson, M.P. Pressure-induced changes in the solution structure of the GB1 domain of protein G. *Proteins Struct. Funct. Bioinform.* **2008**, *71*, 1432–1440.
40. Wilton, D.J.; Ghosh, M.; Chary, K.; Akasaka, K.; Williamson, M.P. Structural change in a B-DNA helix with hydrostatic pressure. *Nucleic Acids Res.* **2008**, *36*, 4032–4037.
41. Chalikian, T.V.; Sarvazyan, A.P.; Plum, G.E.; Breslauer, K.J. Influence of base composition, base sequence, and duplex structure on DNA hydration: apparent molar volumes and apparent molar adiabatic compressibilities of synthetic and natural DNA Duplexes at 25. degree. *C. Biochemistry* **1994**, *33*, 2394–2401.
42. Lin, M.-C.; Eid, P.; Wong, P.T.; Macgregor, R.B. High pressure fourier transform infrared spectroscopy of poly (dA) poly (dT), poly (dA) and poly (dT). *Biophys. Chem.* **1999**, *76*, 87–94.
43. Chalikian, T.V.; Völker, J.; Plum, G.E.; Breslauer, K.J. A more unified picture for the thermodynamics of nucleic acid duplex melting: A characterization by calorimetric and volumetric techniques. *Proc. Natl. Acad. Sci. USA* **1999**, *96*, 7853–7858.
44. Rayan, G.; Macgregor, R.B. Comparison of the heat-and pressure-induced helix-coil transition of two DNA copolymers. *J. Phys. Chem. B* **2005**, *109*, 15558–15565.
45. Dubins, D.N.; Lee, A.; Macgregor, R.B.; Chalikian, T.V. On the stability of double stranded nucleic acids. *J. Am. Chem. Soc.* **2001**, *123*, 9254–9259.
46. Macgregor, R.B. Chain length and oligonucleotide stability at high pressure. *Biopolymers* **1996**, *38*, 321–328.

47. Rougee, M.; Faucon, B.; Mergny, J.; Barcelo, F.; Giovannangeli, C.; Garestier, T.; Helene, C. Kinetics and thermodynamics of triple-helix formation: Effects of ionic strength and mismatched. *Biochemistry* **1992**, *31*, 9269–9278.
48. Lin, M.-C.; Macgregor, R.B. Activation volume of DNA duplex formation. *Biochemistry* **1997**, *36*, 6539–6544.
49. Lin, M.-C.; Macgregor, R.B. The activation volume of a DNA helix-coil transition. *Biochemistry* **1996**, *35*, 11846–11851.
50. Lin, M.C.; Macgregor, R.B. Pressure-jump relaxation kinetics of a DNA triplex helix-coil equilibrium. *Biopolymers* **1997**, *42*, 129–132.
51. Dubins, D.N.; Macgregor, R.B. Volumetric properties of the formation of double stranded DNA: A nearest-neighbor analysis. *Biopolymers* **2004**, *73*, 242–257.
52. Sugimoto, N.; Nakano, S.-I.; Katoh, M.; Matsumura, A.; Nakamuta, H.; Ohmichi, T.; Yoneyama, M.; Sasaki, M. Thermodynamic parameters to predict stability of RNA/DNA hybrid duplexes. *Biochemistry* **1995**, *34*, 11211–11216.
53. Freier, S.M.; Kierzek, R.; Jaeger, J.A.; Sugimoto, N.; Caruthers, M.H.; Neilson, T.; Turner, D.H. Improved free-energy parameters for predictions of RNA duplex stability. *Proc. Natl. Acad. Sci. USA* **1986**, *83*, 9373–9377.
54. SantaLucia, J.; Allawi, H.T.; Seneviratne, P.A. Improved nearest-neighbor parameters for predicting DNA duplex stability. *Biochemistry* **1996**, *35*, 3555–3562.
55. Till, M.S.; Ullmann, G.M. McVol-A program for calculating protein volumes and identifying cavities by a Monte Carlo algorithm. *J. Mol. Model.* **2010**, *16*, 419–429.
56. Connolly, M.L. Solvent-Accessible surfaces of proteins and nucleic acids. *Science* **1983**, *221*, 709–713.
57. Richards, F.M. Areas, volumes, packing and protein structure. *Annu. Rev. Biophys. Bioeng.* **1977**, *6*, 151–76.
58. Richards, F.M. Calculation of molecular volumes and areas for structures of known geometry. *Methods Enzymol.* **1985**, *115*, 440–464.
59. Robinson, C.R.; Sligar, S.G. Hydrostatic pressure reverses osmotic pressure effects on the specificity of EcoRI-DNA interactions. *Biochemistry* **1994**, *33*, 3787–3793.
60. Lynch, T.W.; Kosztin, D.; McLean, M.A.; Schulten, K.; Sligar, S.G. Dissecting the molecular origins of specific protein-nucleic acid recognition: Hydrostatic pressure and molecular dynamics. *Biophys. J.* **2002**, *82*, 93–98.
61. Robinson, C.R.; Sligar, S.G. Heterogeneity in molecular recognition by restriction endonucleases: Osmotic and hydrostatic pressure effects on BamHI, Pvu II, and EcoRV specificity. *Proc. Natl. Acad. Sci. USA* **1995**, *92*, 3444–3448.
62. Royer, C.A.; Chakerian, A.E.; Matthews, K.S. Macromolecular binding equilibria in the lac repressor system: Studies using high-pressure fluorescence spectroscopy. *Biochemistry* **1990**, *29*, 4959–4966.
63. Mohana-Borges, R.; Pacheco, A.B.; Sousa, F.J.; Foguel, D.; Almeida, D.F.; Silva, J.L. LexA repressor forms stable dimers in solution the role of specific DNA in tightening protein-protein interactions. *J. Biol. Chem.* **2000**, *275*, 4708–4712.
64. Merrin, J.; Kumar, P.; Libchaber, A. Effects of pressure and temperature on the binding of RecA protein to single-stranded DNA. *Proc. Natl. Acad. Sci. USA* **2011**, *108*, 19913–19918.

65. Miyoshi, D.; Sugimoto, N. G-Quartet, G-Quadruplex, and G-Wire Regulated by Chemical Stimuli. *Methods. Mol. Biol.* **2011**, *749*, 93–104.
66. Gellert, M.; Lipsett, M.N.; Davies, D.R. Helix formation by guanylic acid. *Proc. Natl. Acad. Sci. USA* **1962**, *48*, 2013–2018.
67. Williamson, J.R.; Raghuraman, M.; Cech, T.R. Monovalent cation-induced structure of telomeric DNA: The G-quartet model. *Cell* **1989**, *59*, 871–880.
68. Smith, F.W. Quadruplex structure of Oxytricha telomeric DNA oligonucleotides. *Nature* **1992**, *356*, 164–168.
69. Davis, J.T. G-Quartets 40 Years Later: From 5'-GMP to molecular biology and supramolecular chemistry. *Angew. Chem. Int. Ed.* **2004**, *43*, 668–698.
70. Patel, D.J.; Phan, A.T.; Kuryavyi, V. Human telomere, oncogenic promoter and 5'-UTR G-quadruplexes: Diverse higher order DNA and RNA targets for cancer therapeutics. *Nucleic Acids Res.* **2007**, *35*, 7429–7455.
71. Heddi, B.; Phan, A.T. Structure of human telomeric DNA in crowded solution. *J. Am. Chem. Soc.* **2011**, *133*, 9824–9833.
72. Zhang, D.-H.; Fujimoto, T.; Saxena, S.; Yu, H.-Q.; Miyoshi, D.; Sugimoto, N. Monomorphic RNA G-quadruplex and polymorphic DNA G-quadruplex structures responding to cellular environmental factors. *Biochemistry* **2010**, *49*, 4554–4563.
73. Williamson, J.R. G-Quartet structures in telomeric DNA. *Annu. Rev. Biophys. Biomol. Struct.* **1994**, *23*, 703–730.
74. Petraccone, L.; Spink, C.; Trent, J.O.; Garbett, N.C.; Mekmaysy, C.S.; Giancola, C.; Chaires, J.B. Structure and stability of higher-order human telomeric quadruplexes. *J. Am. Chem. Soc.* **2011**, *133*, 20951–20961.
75. Todd, A.K.; Johnston, M.; Neidle, S. Highly prevalent putative quadruplex sequence motifs in human DNA. *Nucleic Acids Res.* **2005**, *33*, 2901–2907.
76. Huppert, J.L.; Balasubramanian, S. G-Quadruplexes in promoters throughout the human genome. *Nucleic Acids Res.* **2007**, *35*, 406–413.
77. Endoh, T.; Kawasaki, Y.; Sugimoto, N. Translational halt during elongation caused by G-quadruplex formed by mRNA. *Methods* **2013**, in press.
78. Endoh, T.; Kawasaki, Y.; Sugimoto, N. Stability of RNA quadruplex in open reading frame determines proteolysis of human estrogen receptor  $\alpha$ . *Nucleic Acids Res.* **2013**, in press.
79. Moyzis, R.K.; Buckingham, J.M.; Cram, L.S.; Dani, M.; Deaven, L.L.; Jones, M.D.; Meyne, J.; Ratliff, R.L.; Wu, J.-R. A highly conserved repetitive DNA sequence, (TTAGGG) $_n$ , present at the telomeres of human chromosomes. *Proc. Natl. Acad. Sci. USA* **1988**, *85*, 6622–6626.
80. Zahler, A.M.; Williamson, J.R.; Cech, T.R.; Prescott, D.M. Inhibition of telomerase by G-quartet DNA structures. *Nature* **1991**, *350*, 718–720.
81. Yaku, H.; Fujimoto, T.; Murashima, T.; Miyoshi, D.; Sugimoto, N. Phthalocyanines: A new class of G-Quadruplex-Ligands with many potential applications. *Chem. Commun.* **2012**, *48*, 6203–6216.
82. Cahoon, L.A.; Seifert, H.S. An alternative DNA structure is necessary for pilin antigenic variation in *Neisseria gonorrhoeae*. *Science* **2009**, *325*, 764–767.
83. Cheung, I.; Schertzer, M.; Rose, A.; Lansdorp, P.M. Disruption of dog-1 in *Caenorhabditis elegans* triggers deletions upstream of guanine-rich DNA. *Nat. Genet.* **2002**, *31*, 405–409.

84. Rodriguez, R.; Miller, K.M.; Forment, J.V.; Bradshaw, C.R.; Nikan, M.; Britton, S.; Oelschlaegel, T.; Xhemalce, B.; Balasubramanian, S.; Jackson, S.P. Small-molecule-induced DNA damage identifies alternative DNA structures in human genes. *Nat. Chem. Biol.* **2012**, *8*, 301–310.
85. Siddiqui-Jain, A.; Grand, C.L.; Bearss, D.J.; Hurley, L.H. Direct evidence for a G-quadruplex in a promoter region and its targeting with a small molecule to repress c-MYC transcription. *Proc. Natl. Acad. Sci. USA* **2002**, *99*, 11593–11598.
86. Hazel, P.; Huppert, J.; Balasubramanian, S.; Neidle, S. Loop-Length-Dependent folding of G-quadruplexes. *J. Am. Chem. Soc.* **2004**, *126*, 16405–16415.
87. Rachwal, P.A.; Brown, T.; Fox, K.R. Effect of G-tract length on the topology and stability of intramolecular DNA quadruplexes. *Biochemistry* **2007**, *46*, 3036–3044.
88. Kankia, B.I.; Marky, L.A. Folding of the thrombin aptamer into a G-quadruplex with  $\text{Sr}^{2+}$ : Stability, heat, and hydration. *J. Am. Chem. Soc.* **2001**, *123*, 10799–10804.
89. Olsen, C.M.; Marky, L.A. Energetic and hydration contributions of the removal of methyl groups from thymine to form uracil in G-quadruplexes. *J. Phys. Chem. B* **2008**, *113*, 9–11.
90. Miyoshi, D.; Karimata, H.; Sugimoto, N. Hydration regulates thermodynamics of G-quadruplex formation under molecular crowding conditions. *J. Am. Chem. Soc.* **2006**, *128*, 7957–7963.
91. Yu, H.; Gu, X.; Nakano, S.-I.; Miyoshi, D.; Sugimoto, N. Beads-on-a-string structure of long telomeric DNAs under molecular crowding conditions. *J. Am. Chem. Soc.* **2012**, *134*, 20060–20069.
92. Fan, H.Y.; Shek, Y.L.; Amiri, A.; Dubins, D.N.; Heerklotz, H.; Macgregor, R.B., Jr.; Chalikian, T.V. Volumetric characterization of sodium-induced G-quadruplex formation. *J. Am. Chem. Soc.* **2011**, *133*, 4518–4526.
93. Wang, Y.; Patel, D.J. Solution structure of the human telomeric repeat d[AG<sub>3</sub>(T<sub>2</sub>AG<sub>3</sub>)<sub>3</sub>] G-tetraplex. *Structure* **1993**, *1*, 263–282.
94. Edward, J.T.; Farrell, P.G. Relation between van der Waals and partial molal volumes of organic molecules in water. *Can. J. Chem.* **1975**, *53*, 2965–2970.
95. Kharakoz, D. Partial molar volumes of molecules of arbitrary shape and the effect of hydrogen bonding with water. *J. Solut. Chem.* **1992**, *21*, 569–595.
96. Likhodi, O.; Chalikian, T.V. Partial molar volumes and adiabatic compressibilities of a series of aliphatic amino acids and oligoglycines in D<sub>2</sub>O. *J. Am. Chem. Soc.* **1999**, *121*, 1156–1163.
97. Conway, B. The evaluation and use of properties of individual ions in solution. *J. Solut. Chem.* **1978**, *7*, 721–770.
98. Chalikian, T.V. Structural thermodynamics of hydration. *J. Phys. Chem. B* **2001**, *105*, 12566–12578.
99. Takahashi, S.; Sugimoto, N. Effect of pressure on the stability of G-quadruplex DNA: Thermodynamics under crowding conditions. *Angew. Chem. Int. Ed.* **2013**, in press.
100. Zimmerman, S.B.; Minton, A.P. Macromolecular crowding: Biochemical, biophysical, and physiological consequences. *Annu. Rev. Biophys. Biomol. Struct.* **1993**, *22*, 27–65.
101. Minton, A.P. The influence of macromolecular crowding and macromolecular confinement on biochemical reactions in physiological media. *J. Biol. Chem.* **2001**, *276*, 10577–10580.
102. Ellis, R.J.; Minton, A.P. Join the crowd. *Nature* **2003**, *425*, 27–28.
103. Nakano, S.; Karimata, H.; Ohmichi, T.; Kawakami, J.; Sugimoto, N. The effect of molecular crowding with nucleotide length and cosolute structure on DNA duplex stability. *J. Am. Chem. Soc.* **2004**, *126*, 14330–14331.

104. Miyoshi, D.; Nakamura, K.; Tateishi-Karimata, H.; Ohmichi, T.; Sugimoto, N. Hydration of watson-crick base pairs and dehydration of hoogsteen base pairs inducing structural polymorphism under molecular crowding conditions. *J. Am. Chem. Soc.* **2009**, *131*, 3522–3531.
105. Macaya, R.F.; Schultze, P.; Smith, F.W.; Roe, J.A.; Feigon, J. Thrombin-Binding DNA aptamer forms a unimolecular quadruplex structure in solution. *Proc. Natl. Acad. Sci. USA* **1993**, *90*, 3745–3749.
106. Sasahara, K.; Sakurai, M.; Nitta, K. Volume and compressibility changes for short poly (ethylene glycol)–water system at various temperatures. *Coll. Polym. Sci.* **1998**, *276*, 643–647.
107. Sakurai, M. Partial molar volumes of ethylene glycol and water in their mixtures. *J. Chem. Eng. Data* **1991**, *36*, 424–427.
108. Senior, M.M.; Jones, R.A.; Breslauer, K.J. Influence of loop residues on the relative stabilities of DNA hairpin structures. *Proc. Natl. Acad. Sci. USA* **1988**, *85*, 6242–6246.
109. Varani, G.; Wimberly, B.; Tinoco, I., Jr. Conformation and dynamics of an RNA internal loop. *Biochemistry* **1989**, *28*, 7760–7772.
110. Vallone, P.M.; Paner, T.M.; Hilario, J.; Lane, M.J.; Faldasz, B.D.; Benight, A.S. Melting studies of short DNA hairpins: Influence of loop sequence and adjoining base pair identity on hairpin thermodynamic stability. *Biopolymers* **1999**, *50*, 425–442.
111. Nakano, S.-i.; Hirayama, H.; Miyoshi, D.; Sugimoto, N. Dimerization of nucleic acid hairpins in the conditions caused by neutral cosolutes. *J. Phys. Chem. B* **2012**, *116*, 7406–7415.
112. Chalikian, T.V.; Totrov, M.; Abagyan, R.; Breslauer, K.J. The hydration of globular proteins as derived from volume and compressibility measurements: Cross correlating thermodynamic and structural data. *J. Mol. Biol.* **1996**, *260*, 588–603.
113. Chalikian, T.V. Volumetric properties of proteins. *Annu. Rev. Biophys. Biomol. Struct.* **2003**, *32*, 207–235.
114. Fujimoto, T.; Nakano, S.-I.; Sugimoto, N.; Miyoshi, D. Thermodynamics-Hydration relationships within loops that affect G-quadruplexes under molecular crowding conditions. *J. Phys. Chem. B* **2012**, *117*, 963–972.
115. Garcia, A.E.; Paschek, D. Simulation of the pressure and temperature folding/unfolding equilibrium of a small RNA hairpin. *J. Am. Chem. Soc.* **2008**, *130*, 815–817.
116. Muhuri, S.; Mimura, K.; Miyoshi, D.; Sugimoto, N. Stabilization of three-way junctions of DNA under molecular crowding conditions. *J. Am. Chem. Soc.* **2009**, *131*, 9268–9280.
117. Rajendran, A.; Nakano, S.-I.; Sugimoto, N. Molecular crowding of the cosolutes induces an intramolecular i-motif structure of triplet repeat DNA oligomers at neutral pH. *Chem. Commun.* **2010**, *46*, 1299–1301.
118. Stewart, M.P.; Helenius, J.; Toyoda, Y.; Ramanathan, S.P.; Muller, D.J.; Hyman, A.A. Hydrostatic pressure and the actomyosin cortex drive mitotic cell rounding. *Nature* **2011**, *469*, 226–230.
119. Kappor, S.; Werkmüller, A.; Goody, R.S.; Waldmann, H.; Winter, R. Pressure modulation of ras-membrane interactions and intervesicle transfer. *J. Am. Chem. Soc.* **2013**, *135*, 6149–6156.